Paper No.
16393

Hydrogen embrittlement of Oil Patch Alloy 718 and its correlation to the microstructure

Julia Botinha
VDM Metals International GmbH
Kleffstrasse 23
58762 Altena, Germany

Bodo Gehrmann
VDM Metals International GmbH
Kleffstrasse 23
58762 Altena, Germany

Helena Alves
VDM Metals International GmbH
Kleffstrasse 23
58762 Altena, Germany

ABSTRACT

Alloy UNS N07718 (known as Alloy 718) is a precipitation hardening nickel alloy containing additions of chromium, niobium, titanium, aluminum and molybdenum. This combination of elements provides an alloy with a combination of high yield strength and corrosion resistance required in sour service applications. Through the precipitation hardening heat treatment, the alloy precipitates the intermetallic Gamma Prime (ordered fcc Ni_3Al) and Gamma Double Prime (bcc tetragonal Ni_3Nb) phases, which are responsible for elevating the yield strength of the material. Additionally to the importance of these both phases in the hardening process, previous studies showed that the microstructure of Alloy 718 may also have a direct influence on its susceptibility to Hydrogen Embrittlement.

Laboratory melts with modified compositions based on Alloy UNS N07718 were produced and tested to correlate both mechanical and hydrogen embrittlement properties. The testing plan included mechanical testing, Slow Strain Rate Tensile (SSRT) tests under cathodic protection and numerical thermodynamic simulations.

Key words: Nickel alloys, Corrosion Mechanisms, UNS N07718, Alloy 718, Hydrogen Embrittlement, Neutron Diffraction, Hardening Phases, Slow Strain Rate Tensile Test, Oil and Gas industry

INTRODUCTION

Its outstanding mechanical performance and its very good corrosion resistance have turned Alloy UNS N07718 into the most preferred applied nickel alloys in the Oil & Gas industry.[1] However, recent field component failures reported the occurrence of hydrogen embrittlement,[2] which can be a serious limitation to the material application. The continuing development of oil and gas production industry pushes the needs to develop new materials technology for applications involving high temperatures, high pressures and increasingly aggressive service environments.[3]

The outstanding mechanical features of Alloy UNS N07718 are resultant of the precipitation of the intermetallic phases Gamma Prime (ordered fcc Ni_3Al) and Gamma Double Prime (bcc tetragonal Ni_3Nb), which is allowed by the presence of the alloying elements niobium, aluminum and titanium.

Previous studies show that the strengthening phases Gamma Prime and Gamma Double Prime play an important role on the corrosion resistance of the alloy UNS N07718.[4-10] Gosheva et al. have made important contributions clarifying the impact of microstructure on the hydrogen embrittlement susceptibility of UNS N07718.[8] Their studies concluded that the amount of hydrogen stored in the material during cathodic hydrogen charging was predominantly dependent on the strengthening precipitates and their interface with the Gamma matrix. The precipitates act as trapping sites, slowing down the diffusion process. Klapper et al. showed that the amount and size of precipitates such as Gamma Prime and Gamma Double Prime, as well as the Delta phase, rather than the strength or hardness level only, predominantly affected the hydrogen embrittlement susceptibility and defined the type of embrittlement mechanism.[9] According to his studies, HEDE- (Hydrogen Enhanced Decohesion) and HELP (Hydrogen Enhanced Localized Plasticity)-assisted shear localization may occur on oil-patch N07718 depending on the amount and localization of Delta phase.

Higher volume fractions of Gamma Double Prime precipitates and / or lower volume fractions of Gamma Prime precipitates were reported to have deleterious effects on the hydrogen embrittlement resistance.[10]

Even with the variation of the hardening temperatures, as investigated on previous studies,[4-10] material with significantly differences in the volume fractions of Gamma Prime and Gamma Double Prime precipitates cannot be produced. To reach significant differences in the volume fractions of both hardening phases, adaptations must be made on the chemical composition, since TTT Diagrams available in the literature show that the curves representing the formation of Gamma Prime and

Gamma Double Prime in alloy UNS N07718 overlap.[11] In this context, model alloys with chemical-compositions based on Alloy UNS N07718 were developed, with the aim of producing alloys containing as much Gamma Prime as possible and alloys containing as much Gamma Double Prime as possible. The model alloys were then tested on SSRT tests under cathodic polarization in order to assess the hydrogen embrittlement susceptibility, so that it was possible to correlate the effect of each phase separately to the embrittlement phenomena.

EXPERIMENTAL PROCEDURE

Material

Four laboratory heats were melted in a Vacuum-Induction-Melting (VIM) laboratory furnace with nominal chemical composition as shown in **Table 1**, where the intentionally modified elements are underlined and in bold. The API(1) 6ACRA[12] composition limits are shown in this table for reference. The ingots were homogenized and hot rolled to sheets with 15 mm (0.6 inch) thickness, which were then solution annealed and age hardened according to the parameters given in **Table 2**.

The solution annealing and hardening temperatures were defined firstly by thermodynamic simulations and were then experimentally confirmed. Due to the absence of Aluminum, the Heat C required a higher annealing temperature for solution. After solution annealing the microstructures were checked for recrystallization using optical microscopy and all heats were 100% recrystallized. The hardening temperatures were chosen to be those that experimentally resulted in the greatest hardening, given a single-step heat treatment cycle.

Thermodynamic Simulations

The occurring phases expected after submitting the alloys to different hardening temperatures and their fractions were calculated for the different alloy variations using the Materials Property Simulation Package JMatPro(2) Version 10.0 from Thermotech,[13] with set cooling rate of 3 °C/s.

Microstructure

Samples of each laboratory heat were polished and etched with Kallings 2. Microstructural micrographs of the transversal section were obtained by means of Scanning Electron Microscopy (SEM) in order to check precipitation. SEM was operated at 10 kV accelerating voltage and the free working distance was around 5 mm.

(1) American Petroleum Institute (API), Washington, D.C., USA
(2) Trade name. Java-based Materials Properties.

Table 1

Nominal chemical composition of laboratory heats in wt.-%

Element	Heat A	Heat B	Heat C	Heat D	API 6ACRA composition limits
C	0.015	0.014	0.014	0.014	0.045 max
S	0.0032	0.0032	0.003	0.0025	0.010 max
Cr	18.49	18.54	18.53	18.55	17.0 to 21.0
Ni	53.6	54.1	53.69	53.77	50.0 to 55.0
Mn	0.01	0.01	0.01	0.01	0.35 max
Si	0.03	0.02	0.03	0.02	0.35 max
Mo	3.05	2.95	3.05	3.02	2.80 to 3.30
Ti	0.95	0.9	0.94	0.93	0.80 to 1.15
Nb + Ta	4.89	**0.02**	5.2	**3.55**	4.87 to 5.20
Cu	0.01	0.01	0.01	0.01	0.23 max
Fe (R)	18.37	22.86	18.53	19.5	Balance
P	0.003	0.003	0.003	0.003	0.010 max
Al	0.51	0.51	**0.01**	0.54	0.40 to 0.60
Mg	0.001	0.001	0.001	0.001	0.0060 max
Ca	0.001	0.001	0.001	0.001	0.0030 max
Co	0.01	0.01	0.01	0.01	1.00 max
B	0.005	0.004	0.005	0.004	0.0060 max

Table 2

Heat treatment parameters of laboratory heats

Heat	Solution annealing			Age hardening		
	Temp [°C (°F)]	Time [h]	Cooling media	Temp [°C (°F)]	Time [h]	Cooling media
A	1032 (1890)	2	Water	760 (1400)	7	Air
B	1032 (1890)	2	Water	770 (1418)	7	Air
C	1045 (1913)	2	Water	770 (1418)	7	Air
D	1032 (1890)	2	Water	750 (1382)	7	Air

Mechanical Properties

Tensile, Charpy impact and hardness tests were carried out in all model alloys to check for mechanical properties.

Tensile test was conducted at room temperature according to ASTM[3] E8[14] on round tensile M10 samples on the transverse direction to the rolling direction.

Charpy specimens with notch in the longitudinal direction were tested at a temperature of -60 °C (-75 °F) according to ASTM E23[15].

Rockwell hardness (HRC) readings were performed according to DIN EN ISO [4]6508[16] in three different positions in the half-thickness of the material.

Hydrogen Embrittlement Susceptibility Test

In order to evaluate the hydrogen embrittlement susceptibility of the laboratory heats, SSRT tests were carried out with test specimens complying with NACE[(5)] TM0198-2011,[17] having a gauge section diameter of 3.81 mm (0.15-in) and length of 25.4 mm (1-in). For each laboratory heat, one specimen was tested in a control environment, which consisted of distilled water purged with nitrogen, and three specimens were tested in an aggressive environment, which consisted of 0.5 M sulfuric acid solution with applied cathodic current density of 5 $mA \cdot cm^{-2}$. Water was selected as the control environment, due to its inertness and the better temperature control in comparison to other media such as glycerol and air. No reaction was expected between the distilled water and the material surface. Both solutions were maintained at the temperature of 40°C (104°F) during the tests and the specimens were submitted to a strain rate of $1x10^{-6}$ s^{-1} (crosshead speed $2.5x10^{-5}$ $mm \cdot s^{-1}$). Elongation-to-failure, plastic elongation, time-to-failure and tensile-strain were reported, as well as the ratios of these values between aggressive and control environments.

A set threshold of 45% for elongation ratio between inert/aggressive environments is used to qualify Alloy UNS N07718 material as acceptable or not acceptable resistance against hydrogen embrittlement.[18] Elongation ratios greater than 45% are considered acceptable and the higher this value, the less the susceptibility of a material to hydrogen embrittlement.

(3) American Society for Testing and Materials (ASTM), West Conshohocken, Pennsylvania, USA
(4) International Organization for Standardization (ISO), Geneva, Switzerland
(5) National Association of Corrosion Engineers (NACE) International, 15835 Park Ten Place, Houston, TX 77084

RESULTS AND DISCUSSION

Thermodynamic Simulations

The occurring phases and their fractions in wt.% after age hardening at the temperature corresponding to the greatest hardening, when the material has the higher mechanical properties, were calculated for the different alloy compositions. The calculated fraction of the hardening phases precipitated in each alloy is summarized on **Table 3.**

The numerically calculated fractions of Gamma Prime and Gamma Double Prime phases in the reference composition (corresponding to the reference laboratory heat A) are comparable to values from previous studies. Botinha et al. demonstrated, by means of neutron diffraction methods, that Alloy UNS N07718, when age hardened at 760 °C (1400 °F), the known temperature for peak mechanical properties, precipitates fractions of Gamma Prime and Gamma Double Prime both in the order of 13%,[10] and comparable results are reported here.

Table 3

Numerically calculated fraction of Gamma Prime and Gamma Double Prime precipitates present for each alloy composition

Heat	A	B	C	D
Fraction of Gamma Prime [%]	9.26	4	3.87	9.02
Fraction of Gamma Double Prime [%]	8.5	0	11.47	4.34

As expected, heat B, which does not have niobium additions, should precipitate only Gamma Prime, since the presence of only aluminum and titanium as hardening-phase-formation elements should favor the formation of Gamma Prime phase. However, annulling the content of niobium and considering that the existing aluminum content on the reference material is already low (in the range of 0.5%), a very low quantity of 4% Gamma Prime is expected to precipitate.

According to the calculations, heat C precipitates mainly Gamma Double Prime with a much lower fraction of Gamma Prime, since Gamma Double Prime is mainly formed by the combination between niobium and nickel. The small fraction of Gamma Prime phase expected to form on heat C is due to the substitution of aluminum atoms by titanium and a small fraction of niobium for the formation of the fcc Gamma Prime phase.

In order to produce materials with comparable precipitation scenarios, a fourth variation with reduced niobium content was melted (heat D). With a niobium content reduced to around 3.5%, heat D contains

both Gamma Prime and Gamma Double Prime precipitates, but in quantities opposite to in heat C, which allows a more suitable evaluation of the response of each phase to the hydrogen embrittlement.

Neutron Diffraction techniques were carried out in the Heinz Maier-Leibnitz Zentrum (MLZ), part of the Technical University of Munich, in order to identify the different phases present in the samples and their weight fractions (wt.%). The experimentally obtained wt.% of Gamma Prime and Gamma Double Prime phases are very similar to the values expected from thermodynamic calculations. The most relevant deviation is regarding the Gamma Double Prime content of heat A, which experimentally was measured lower than as expected by the calculations. Due to the isolated and overlapping peaks of Gamma Double Prime in the Neutron Diffraction (ND) patterns, the characterization of this phase can be very challenging and lead to reasonable scatter.

Microstructure

Transverse micrographs showing the present precipitates obtained by SEM are shown in **Figures 1 to 4**. For each laboratory heat, micrographs of the representative bulk phases at 50k and 30k magnification were produced.

The identification of both Gamma Prime and Gamma Double Prime phases through SEM images is difficult and therefore the SEM analysis are shown for relative reference. Gamma Prime particles are known to precipitate with a point-shape while Gamma Double Prime particles usually present a linear shape. An attempt to exemplify the both particle formats was made on Figure 1 by the use of yellow arrows.

High temperature phase expected to be Delta phase was detected on grain boundaries of heat C (Figure 3), what was attributed to the higher availability of niobium in the matrix. Thermodynamic calculations indicate that the grain boundary precipitate may be Delta phase, but this was not confirmed by any other method of analysis. Please note that the decorated grain boundary showed on Figure 3 is not representative of the whole sample and was presented here to illustrate the regions where dense grain boundary decoration can be seen.

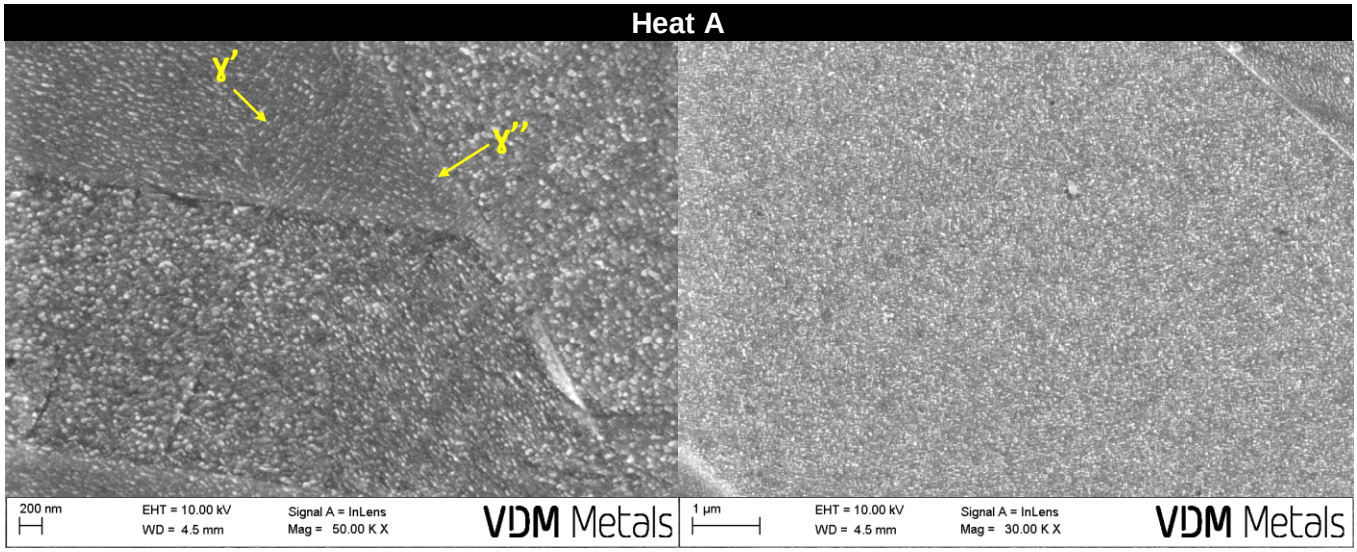

Figure 1: SEM images of laboratory heat A (reference) showing the precipitates after age hardening at 760 °C for 7 hours.

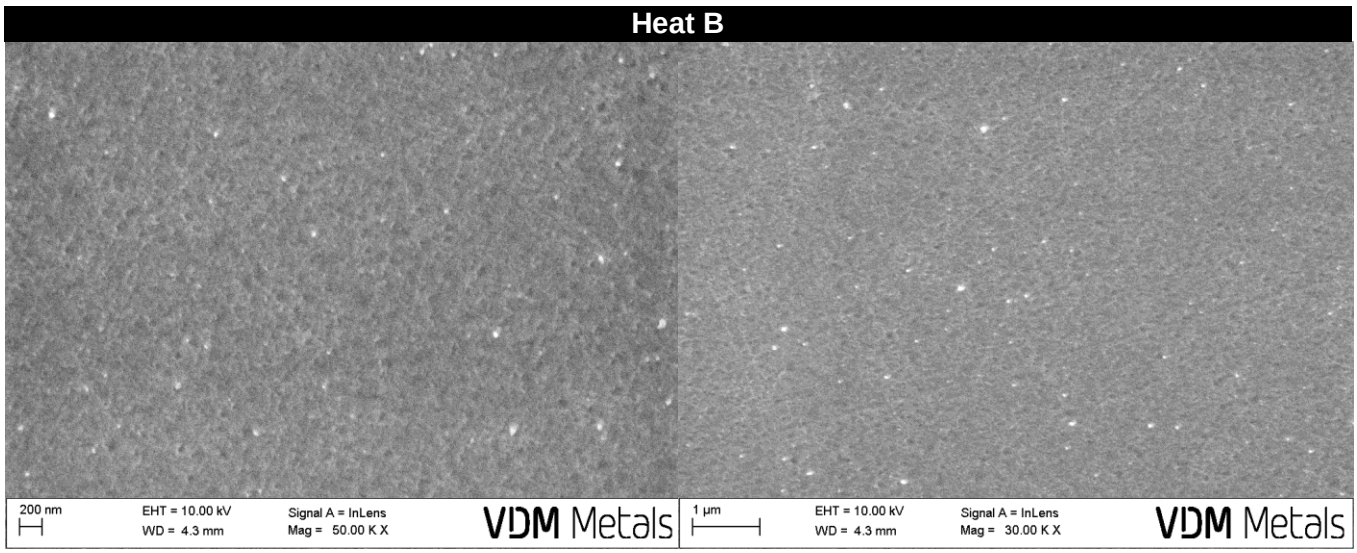

Figure 2: SEM images of laboratory heat B (without Nb) showing the precipitates after age hardening at 770 °C for 7 hours.

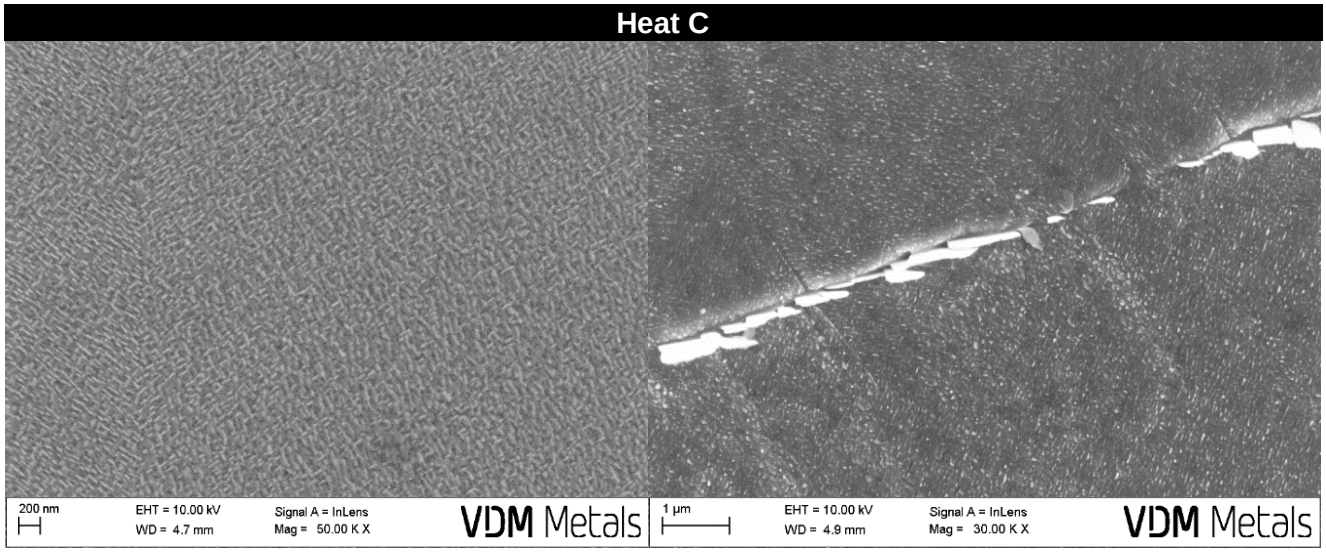

Figure 3: SEM images of laboratory heat C (without Al) showing the precipitates after age hardening at 770 °C for 7 hours.

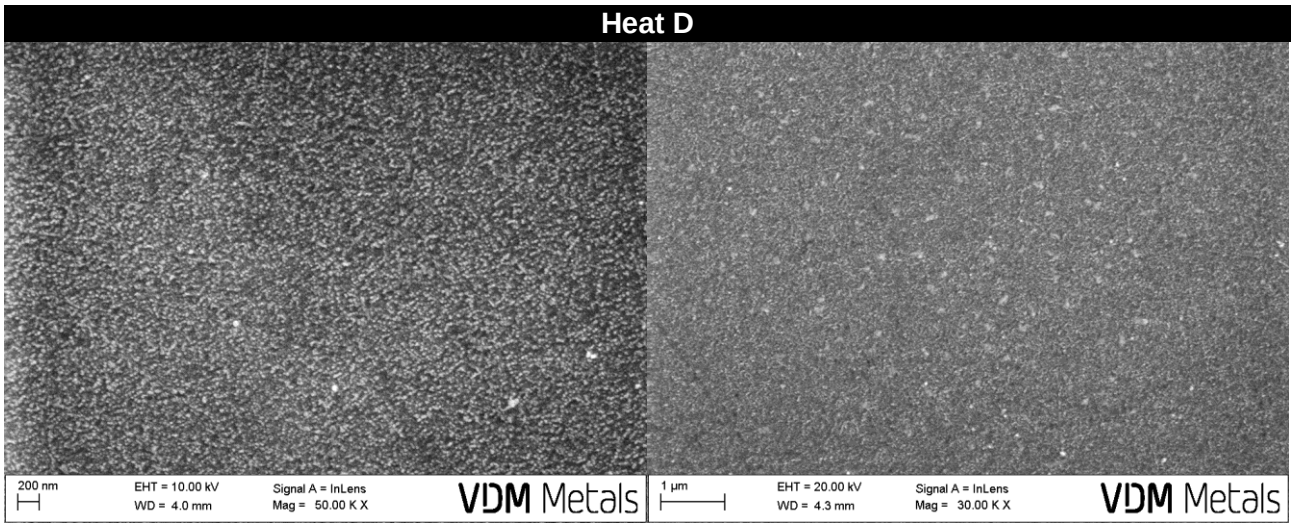

Figure 4: SEM images of laboratory heat D (low Nb) showing the precipitates after age hardening at 750 °C for 7 hours.

Mechanical Properties

Tensile properties, impact energy and hardness of the tested model alloys are shown on **Table 4**. As expected, lower niobium contents result in lower yield strength, hardness, and impact toughness.

Heat A, the reference, has mechanical properties that are lower compared to standard mill-produced UNS N07718 according to the API 6ACRA 140K Material Designation. This feature can be explained by

the low niobium content of heat A that lies on the lowest permitted range, fact that can contribute to the lower mechanical properties presented by this heat in comparison to mill-manufactured usual properties.

Table 4

Mechanical Properties of model alloys based on Alloy UNS N07718

Heat	Comment	Rp0,2		Rp0,1		Rm		A*	Z	Charpy Impact -60 °C	Härte HRC			
		MPa	ksi	MPa	ksi	MPa	ksi	%	%	J	M1	M2	M3	Av.
A	Ref.	833	121	954	138	1185	172	29	39	76	39 37	37 37	37 38	38
B	w/o Nb	249	36	286	41	623	90	54	44	194	<20	<20	<20	<20
C	w/o Al	944	137	1035	150	1226	178	25	36	56	39	40	39	40
D	low Nb	684	99	745	108	1032	150	39	55	111	29	29	30	29

The heat B presents the lowest tensile and hardness properties together with the highest ductility. The hardening effect seems to be not guaranteed by the precipitation of very low amounts of Gamma Prime and absence of Gamma Double Prime. The mechanical properties of heat C can be compared to solution annealed material.

Heat C, without aluminum, has the highest tensile and hardness properties and poorest ductility levels when compared to the other three heats, likely due to the preferential precipitation of Gamma Double Prime.

On the other hand, although having more Gamma Prime precipitation and reduced Gamma Double Prime, heat D presents unique mechanical properties, with hardness, yield and tensile strengths slightly lower when compared to heat A, but with much higher ductility.

Hydrogen Embrittlement Susceptibility Test

The susceptibility of the alloys to hydrogen embrittlement was evaluated by means of SSRT. When comparing the ductility parameters determined for the samples tested in aggressive environment with those of samples tested in control (inert) environment, ductility ratios were calculated and the loss in ductility was used to rate the resistance to the embrittlement caused by the hydrogen. The lower the plastic elongation ratio, the higher the sensitivity to hydrogen embrittlement. Detailed SSRT results are presented on **Table 5**, where ETF is the elongation-to-failure measured experimentally on the testing sample, Ep is the plastic elongation calculated using Equation 3 from NACE TM0198, TTF is the time-to-failure and Rm is the tensile strength. **Figure 5** shows a diagram for comparison of the average

plastic elongation ratios of the different alloy compositions to the elongation ratios of Alloy UNS N07718 in the 140K material designation, which is available in the literature,[10] when standard production material was tested at the same conditions which were used for the present studies. The values regarding the 140K material designation were selected as a reference for this study, since this is the grade that corresponds to the higher mechanical properties achieved by a single-step age hardening and therefore could be directly compared to the laboratory melts, regarding the heat treatment parameters.

Table 5

Hydrogen embrittlement susceptibility SSRT test results

Heat	Test Environment	Sample-Nr	ETF		Ep		TTF		Rm	
			[%]	Ratio [%]	[%]	Ratio [%]	min	Ratio [%]	MPa	Ratio [%]
A	inert	A1	22.7	-	23.2	-	4887	-	1138	-
	aggressive	A2	13.5	59.5	14.3	61.6	3298	67.5	1118	98.2
	aggressive	A3	13.6	59.9	13.6	58.6	3448	70.6	1092	96.0
	aggressive	A4	12.1	53.3	13.5	58.2	3375	69.1	1062	93.3
		Average		**57.6**		**59.5**		**69.0**		**95.8**
B	inert	B1	40.9	-	49.8	-	9098	-	535	-
	aggressive	B2	44.9	109.8	51.1	102.6	9283	102.0	586	109.5
	aggressive	B3	44.8	109.5	52.2	104.8	9442	103.8	487	91.0
	aggressive	B4	43	105.1	48.8	98.0	9039	99.4	513	95.9
		Average		**108.1**		**101.8**		**101.7**		**98.8**
C	inert	C1	17.7	-	19.6	-	4222	-	1108	-
	aggressive	C2	7.9	44.6	8.4	42.9	2524	59.8	1094	98.7
	aggressive	C3	10.5	59.3	8.0	40.8	2450	58.0	1088	98.2
	aggressive	C4	8	45.2	6.8	34.7	2055	48.7	1038	93.7
		Average		**49.7**		**39.5**		**55.5**		**96.9**
D	inert	D1	30.5	-	33.2	-	6343	-	973	-
	aggressive	D2	28.4	93.1	29.9	90.1	5934	93.6	937	96.3
	aggressive	D3	26.2	85.9	29.6	89.2	5838	92.0	882	90.6
	aggressive	D4	31	101.6	32.2	97.0	6213	98.0	895	92.0
		Average		**93.6**		**92.1**		**94.5**		**93.0**

Heat A, reference laboratory heat, with chemical analysis in accordance to the API 6ACRA for the UNS N07718, presented an average plastic elongation ratio of 59.5%. This value goes well with the expected, given Alloy UNS N07718, aged to the peak of mechanical properties after a single-step ageing (corresponding to the 140K grade of API 6ACRA), presented, in the literature, elongation ratios of around 70%.[10, 19]

The laboratory heat B (without Niobium addition), did not show any susceptibility to Hydrogen Embrittlement, since the plastic elongation ratios are in the order of 100%. This means that the material does not lose ductility after being exposed to the hydrogen charged medium. It is not uncommon that ratios higher than 100% are obtained for materials resistant to Hydrogen Embrittlement, considering the existence of a scattering in the measurements. Test on inert medium was repeated and no deviation from the values of the first sample was observed.

With a chemical composition free of Aluminum, the laboratory heat C is the most susceptible to hydrogen embrittlement, showing plastic elongation ratio of 39.5% in average. Delta phase precipitation was detected on the grain boundaries, what explains the generally reduced ductility of the material, due to the weak interface between precipitate and matrix. However, according to previous studies, an increasing amount of Delta phase on Alloy UNS N07718 (until a number of precipitates >>1 per µm of grain boundary) was not deleterious to the Hydrogen Embrittlement behavior of the material.[9,20] Comparing to the analysis of the cited studies, the quantity of Delta phase on heat C is lower than >>1 particle per µm of grain boundary and therefore, the low elongation ratio was attributed to the amount of Gamma Double Prime phase in this heat.

Heat D presented plastic elongation ratio of 92.1%. The small loss in ductility after exposure to the hydrogen charged medium was correlated to the presence of Gamma Double Prime particles in smaller amounts, when compared to the standard compositions of UNS N07718. This combination of low niobium and usual aluminum content assured an improved resistance against Hydrogen Embrittlement while maintaining good mechanical properties and ductility.

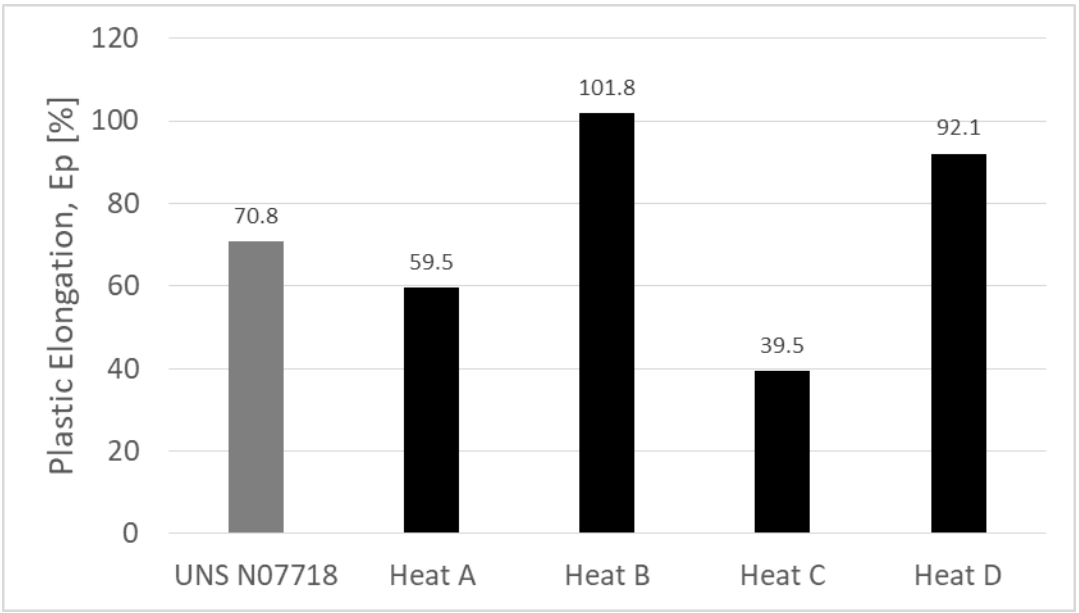

Figure 5: Plastic Elongation ratio of model alloys in comparison to production heat of Alloy UNS N07718 in the 140K Material Designation available in the literature [10]

Taking in consideration the both reference values for Alloy UNS N07718 – the production heat in the 140K grade from the literature[10] and the reference laboratory heat A – and comparing it with the characteristics of the laboratory heats B, C and D, it can be assumed that the higher the proportion Gamma Prime / Gamma Double Prime, the higher the resistance of the alloys to hydrogen embrittlement.

CONCLUSIONS

Model alloys with microstructures containing more of one or another hardening phase, i.e. Gamma Prime and Gamma Double Prime, allowed the confirmation of the theory developed on previous works that the hardening phases play an important role on the Hydrogen Embrittlement resistance of Alloy UNS N07718.

It could be concluded that the ordered fcc Gamma Prime phase was not responsible for the embrittlement of the model alloys, since material presenting only this phase on the microstructure did not present any reduction in ductility after being strained under the aggressive environment. Additionally, materials with a high fraction of Gamma Prime presented less susceptibility to Hydrogen Embrittlement than materials in the opposite condition, which have a lower fraction of Gamma Prime.

However, the results showed that the bcc tetragonal Gamma Double Prime phase may play an important role on the embrittlement of alloy UNS N07718. The ductility of material containing mainly Gamma Double Prime phase on its microstructure (Heat C, although presenting also Delta phase decoration on grain boundaries) greatly decreases after being strained under aggressive environment, and as the amount of Gamma Double Prime phase was reduced, as on heat D, an increase of elongation ratios was seen.

While Gamma Double Prime, that precipitates from higher niobium contents, increase susceptibility for embrittlement, it is essential in achieving higher strength levels. Only Gamma Prime in the low amounts achieved by heat B was insufficient to elevate the strength and hardness.

The presence of intergranular precipitation can be detrimental to the mechanical and corrosion properties, although these studies did not allow their correlation to the tensile properties and the susceptibility to Hydrogen Embrittlement.

AKNOWLEDGEMENTS

The authors would like to thank Fabian Ramlau for the good work to produce SEM micrographs within the labs of VDM Metals. Further thanks to the Salzgitter Mannesmann Research Institute for carrying out SSRT corrosion tests and to the MLZ in the University of Munich for the support with the neutron diffraction measurements and evaluation.

REFERENCES

1. U. Heubner, J. Kloewer, Nickelwerkstoffe und hochlegierte Sonderedelstähle: Eigenschaften – Verarbeitung – Anwendungen, 4th ed. (Renningen, 2009)
2. S.Huizinga, B. McLoughlin, W.E. Like and J.G. de Jong. “Offshore nickel alloy tubing hanger and duplex stainless steel piping failure investigations”, NACE Corrosion 2003, Paper no. 03129 (Houston, USA: NACE, 2003)
3. R. Kane, M. Cayard, Roles of H2S in the behavior of engineering Alloys: a Review of Literature and Experience, CORROSION/98, paper no. 274 (Houston, TX: NACE, 1998)
4. B. Kagay, K. Findley, S. Coryell, A.B. Nissan, “Effects of alloy 718 microstructure on hydrogen embrittlement susceptibility for oil and gas environments”, Material Science and Technology Vol. 32, No 7-8 (2016): 697-707.
5. L. Liu, K. Tanaka, A. Hirose, K. F. Kobayashi, “Effects of precipitation phases on the hydrogen embrittlement sensitivity of Inconel 718,” Science and Technology of Advanced Materials 3 (2002): 335-344.
6. Z. Guo, M. Zhao, C, Li, S. Chen, L. Rong, Mechanism of hydrogen embrittlement in a gamma-prime phase strengthened Fe-Ni based austenitic alloy”, Elsevier, Materials Science and Engineering A 555 (2012) 77-84
7. M. C. Rezende, L. S. Araujo, S. B. Gabriel, D. S. dos Santos, L. H. de Almeida, “Hydrogen embrittlement in nickel-based superalloy 718: Relationship between γ´+ γ´´ precipitation and the fracture mode,” International Journal of Hydrogen Energy 40 (2015): 17075-17083
8. O. Gosheva, G. Anderson, M. Oechsner, J. Klöwer, A. Aghajani, “Impact of microstructure on hydrogen solubility and diffusivity in UNS 07718”, CORROSION/2016, paper no. 7267 (Houston, TX: NACE 2016)
9. Sarmiento Klapper H, Klöwer J, Gosheva O. 2017 Hydrogen embrittlement: the game changing factor in the applicability of nickel alloys in oilfield technology. Phil. Trans. R. Soc. A 375: 20160415.
10. J. Botinha, B. Gehrmann, H. Alves, R. Gilles, C. Solís, J. Munke, A. Feoktystov, V. Baran. “Study of Phase Distribution on Alloy UNS N07718 in Different Hardening Conditions and its Relationship with Hydrogen Embrittlement Susceptibility”. NACE Corrosion 2019, Paper no. 13025 (Houston, USA: NACE, 2019)
11. A. Oradei-Basile and J.F Radavich, “A Current T-T-T Diagram for Wrought Alloy 718” Superalloys 718, 625 and Various Derivatives, Edited by Edward A. Loria. The Minerals, Metals & Materials Society, 1991.
12. API Standard 6ACRA, First Edition (August 2015), “Age-hardened Nickel-based Alloys for Oil and Gas Drilling and Production Equipment” (Washington, NW: API Publishing Services).
13. N. Saunders, Z. Guo, X. Li, A. P. Miodownik and J-Ph. Schillé, “Modelling the Material Properties and Behaviour of Ni-Based Supperalloys”. Superalloys 2004, TMS (the Minerals, Metals & Materials Society), 2004.
14. ASTM E8 / E8M-16ae1, Standard Test Methods for Tension Testing of Metallic Materials, ASTM International, West Conshohocken, PA, 2016, www.astm.org
15. ASTM E23-18, Standard Test Methods for Notched Bar Impact Testing of Metallic Materials, ASTM International, West Conshohocken, PA, 2018, www.astm.org

16. DIN EN ISO 6508-1:2016-12, Metallic materials - Rockwell hardness test - Part 1: Test method (ISO 6508-1:2016); German version EN ISO 6508-1:2016
17. NACE TM0198-2011, “Slow Strain Rate Test Method for Screening Corrosion-Resistant Alloys (CRAs) for Stress Corrosion Cracking in Sour Oilfield Service”, (Houston, TX: NACE International)
18. L. Foroni, “Hydrogen Embrittlement Susceptibility of Precipitation Hardened Ni-Alloys”, CORROSION/2014, paper no. 3948 (Houston, TX: NACE, 2014).
19. J. Rosenberg, J. Klöwer, J. Groth, C. Bosch, G. Genchev. „Effect of heat treatment on mechanical properties and corrosion resistance of Nickel Alloy UNS N07718 – 140 ksi and 150 ksi grades“. NACE Corrosion 2018, Paper No. 10650 (Houston, USA: NACE, 2018).
20. O. Gosheva, “Effect of the microstructure of nickel alloy UNS N07718 on its corrosion behavior” (doctor thesis, Darmstadt, GE, 2018)